ORIGINAL ARTICLE

Mapping of subsurface structural features in some parts of Anambra Basin, Nigeria, using aeromagnetic data

Bethrand Ekwundu Oguama[1,2] · Francisca Nneka Okeke[1] · Daniel Nnaemeka Obiora[1]

Abstract
Aeromagnetic data of some parts of Anambra Basin, Nigeria, covering Illushi, Nsukka, Igumale, Onitsha, Udi and Nkalagu areas were digitally processed, analyzed and interpreted qualitatively and quantitatively. The study was carried out to delineate the subsurface structural lineaments/trends that provide the locales for mineral deposit and hydrocarbon resources and to estimate the depth to magnetic sources/sedimentary thickness of the area. The data were qualitatively interpreted using reduction to equator-inverted (RTE_INV), vertical derivatives (VD), tilt derivative (TDR) filter, lineament density filter and Rose plot. Quantitative interpretation was done using source parameter imaging and Euler deconvolution methods. The results depicted that the study area has enormous structural lineaments especially in the northeast and northwest that showed a high cluster of these lineaments. The results showed that the trends of the structural lineaments have a dominance of NE–SW direction, with ancillary trends in E–W, NW–SE, N–S, NNE–SSW and ENE–WSW directions. The SPI depth result ranges from 318.45 m for shallow magnetic sources to − 11,253 m for sedimentary thickness. The 3D Euler deconvolution depth estimate revealed depths to magnetic sources ranging from − 400 to − 4300 m. The results show good evidence of the presence of the essential factors for the exploration of both mineral deposits and hydrocarbon resources in the study area.

Keywords Aeromagnetic data · Anambra basin · Euler deconvolution · Hydrocarbon · Lineaments · Source parameter imaging

Introduction

Anambra Basin is classified as having good prospects for oil and gas and indeed other minerals, except for the chance that structures could have been breached or flushed (Whiteman 1982). The possible traps types in Anambra Basin as identified by Whiteman (1982) include anticlines, faults, and unconformities, stratigraphic and burial hills. The suspicion and later discovery of growth faults in a small scale in the outcropping appearances of Nkporo group (Nwajide 2006) is an evidence of structural possibilities in the subsurface of Anambra Basin; which has not been clearly understood.

The inherent genetic ambiguity and structural complexity in the basin has generated a lot of interest amongst geoscientists. Perhaps, the results obtained by previous researchers in attempting to understand and characterize the basin with the utmost aim of assessing its hydrocarbon and solid mineral potentials were limited by the inadequacy of either the data used or the method applied. The high cost of test drilling and other limitations of the use of well log data in assessing the burial history and subsidence of Anambra Basin (Ekine and Onuoha 2008), with a view to determining the structural trends and understanding the structural possibilities call for the use of high-resolution aeromagnetic data and the application of newer methods for possible generation of subtler and better informative results.

Apart from this, further studies of hydrocarbon and mineral potentials of parts of this basin is mainly concentrated at the upper part of the basin that has shown evidence of the presence of intrusive (Ofoegbu 1984; Adetona and Abu 2013; Obiora et al. 2016). However, structural evidences from previous researchers reported that mineralization in the upper part of the basin may be close to the surface, and therefore the deposits are not extensive enough to attract huge investments from big mining companies. In the lower

✉ Daniel Nnaemeka Obiora
  daniel.obiora@unn.edu.ng

[1] Department of Physics and Astronomy, University of Nigeria, Nsukka, Enugu State, Nigeria

[2] Department of Physics Education, Enugu State College of Education (Technical), Enugu State, Nigeria

part of the basin, the zeal for geophysical investigations was slightly shunned perhaps for the lack of interest and subversion of exploratory activities and studies following the discovery of an abundance of hydrocarbon in the neighboring Niger Delta region (Nwajide 2006).

As newer data and tools are generated and developed, it becomes increasingly possible not only to detect deeper and subtle deposits but to model and characterize the basin in terms of the extents of mineralization. These depend so much on the proper knowledge of the geology of the region under study.

Most of the rocks in the earth's subsurface are magnetic in nature. They posses induced magnetization from the earth's magnetic field and/or remnant magnetization acquired sometime in the geologic past. Magnetic survey, therefore, investigates the earth subsurface based on the variations in the earth's magnetic field that results from the magnetic properties of the underlying rocks. Mapping the patterns of the magnetic anomalies provides insight into the earth's subsurface structure. The aeromagnetic survey provides a rapid and comparatively inexpensive approach to regional problems and always helps in selecting the priority areas for further investigations (Farah et al. 2009).

Although, sedimentary rocks and the surface cover formations (including water) are non magnetic, the observed anomalies are attributed to the combined magnetic effects of several magnetic markers of underlying magnetic sources; which include igneous and magnetic basement rocks (Gunn 1995; Adetona and Abu 2013). Thus, the aeromagnetic surveys are able to indicate the distribution of bedrocks lithologies and structures as a result of the anomalies that extended from the source through the sedimentary pile to the magnetometer. Specifically, it can map and interpret faulting, shearing and fracturing as potential hosts of various minerals and an indirect guide to epigenetic, stress-related mineralization of surrounding rocks (Adetona and Abu 2013; Megwara and Udensi 2014). The survey provides insight from which one can determine the depth to basement, and therefore locate and define the extent of sedimentary thickness required for oil and gas prospecting.

Lineaments are the major topographical features or geological structures that can be found in sedimentary, igneous and metamorphic rocks. Analysis of the structural lineament pattern (trend) is an essential tool for understanding the basin development and could provide clearer information on the structural possibilities of the area; as it often indicates the form and position of individual folds, faults, joints, veins, lithologic contacts and other structural features that provide regional structural pattern (Onyewuchi et al. 2012; Megwara and Udensi 2014). A good correlation exists between areas of high lineament density and the areas of occurrence of most primary minerals including gold, iron ore, cassiterite, tantalite, clay and uranium (Ananaba and Ajakaiye 1987; Megwara and Udensi 2014). Areas of lineaments are associated with mostly fracture lines defined by joints that are formed as a result of tensional stresses. They form a network of cross cutting each other and generally decrease in width and size with an increase in depth; because they are sealed up at depth by lithostatic pressure (Ngama and Akanbi 2017). Hence, a good understanding of the structural lineament pattern could provide clearer information on the distribution of structures in Anambra Basin, using high-resolution aeromagnetic data.

Several published works on the interpretation of aeromagnetic data over the entire Anambra Basin and Lower Benue Trough were conducted using different methods (Onwuemesi 1997; Adetona and Abu 2013; Ofoha 2015; Obiora et al. 2015; Ekwueme et al. 2018; Okorie et al. 2019; Yakubu et al. 2020). However, no specific works had been carried out in the present area of study as a sub-region in Anambra Basin. Onwuemesi (1997) employed one-dimensional spectral analysis of aeromagnetic data of Anambra Basin, and determined the sedimentary thickness that varied between 0.9 and 5.6 km. Adetona and Abu (2013) employed both spectral depth method and source parameter imaging (SPI) to investigate the sedimentary thickness and structural trend within Upper Anambra Basin. They revealed a sedimentary thickness for magnetic bodies ranging from 0.07698 to 9.847 km and structural trends in N–E and NE–SW directions.

Study carried out by Ofoha (2015) investigated high-resolution aeromagnetic data to interpret the basement morphology and the structural framework of parts of Anambra Basin, along Mmaku, Ngwo, Ezeagu, Awka, Nanka, Ekwulobia and Oji-River. He delineated structural lineaments that trend in NE–SW, NW–SE, NNE–SSW and N–S directions. Obiora et al. (2015) employed standard Euler deconvoluntion, source parameter imaging (SPI) and forward and inverse modeling techniques to interpret aeromagnetic data over Nsukka area for hydrocarbon exploration. Their results revealed SPI depth range of 151.6–3082.7 m for outcropping, shallow and deep magnetic bodies. They obtained susceptibility values from five model profiles; 0.0031, 0.0073, 1.4493, 0.0069 and 0.0016; which they attributed to the dominance of iron-rich minerals and forms lateritic caps on sandstones. The Euler depth range estimated in their study was 7.99–128.93 m for four different structural indices of the shallow magnetic sources. They concluded that a depth range of 35–150 m was good potential water reservoirs for Nsukka and environs. Also, they reported that a depth range of 1644–3082.7 m showed sufficient thick sediments for hydrocarbon accumulation.

The aeromagnetic data interpretation of Idah and Angba areas (Northern Anambra Basin) carried out by Ekwueme et al. (2018) revealed deep magnetic anomaly sources that vary between 2.194 and 6.764 km and shallow magnetic anomaly sources that vary from 0.597 to 1.592 km. Further,

they employed forward and inverse modeling methods and obtained depth ranging from 461 to 6847 m for five profiles taken in the area. Okorie et al. (2019) carried out a qualitative and quantitative interpretation of aeromagnetic data over Ubiaja and Illushi area in northern Anambra Basin, Nigeria, using combined methods. They reported that the area was vastly faulted with major anomalies (faults) trending in the NE–SW direction. They reported SPI depth that ranged from − 258.2 to − 3497.7 m, Euler deconvolution depth that ranged from 1377.3 to − 3089.9 m (for structural index 0.5, 1, 2, 3) and the forward and inverse modeling depth that ranged between − 2964 and − 5489 m. The work of Yakubu et al. (2020) showed evidence of the possibility of hydrocarbon exploration in Anambra Basin.

In this study, total magnetic intensity, reduction to equator inverse, vertical derivatives, tilt derivative, source parameter imaging and Euler deconvolution methods were employed to study the magnetic lineaments with particular interest on the trends and depth to magnetic sources. The study will provide an insight into the environmental impact assessment of the region, and will also be of great benefit to the exploration industries, government and intending researchers.

Location and geology of the area of study

The study area lies between longitudes 6° 30′ E–8° 00′ E and latitudes 6° 00′ N–7° 00′ N. The area is a sedimentary basin, sandwiched between the Southern Benue Trough and Niger Delta Basin. The area is an elongated NE–SW trends (Aigbogun and Olorunsola 2018) and characterized by hilly and undulating relief especially in the northern and eastern part of the area. The study area covers Enugu, Anambra, some parts of Kogi, Benue, Ebonyi, and Imo States.

The study area is basically a sedimentary basin with thickness ranging from 2.5 to 6 km (Ekweozor 2006), and mature source rocks packaged into Eze-aku group, Awgu formation, Nkporo group, Coal measures, Imo formation and Bende Ameki Group (Fig. 1). The Nkporo group is made up of Nkporo shale, Enugu formation, Owelli sandstones, Otobi sandstones and Lafia sandstones; while Coal Measures are made up of Mamu formation, Ajali formation (sandstone) and Nsukka formation (mainly sandstone and limestone). Mamu formation contains mainly unconsolidated coarse–fine grain, poor cemented, mudstone and siltstone (Adeigbe and Salufu 2009). The area has a large segment of Alluvium and a small portion of coastal plain sands. Also, the Basin has containment subsystems that include anticlines, faults, unconformities and combination traps (Nwajide 2006). Its percentage of lithostratigraphic units comprise 60% shale, 40% sands and less than 1% limestone (Reyment 1965; Nwajide 2006).

The digital elevated model (DEM) of the study area is shown in Fig. 2. DEM is the topographical feature of the study area defined by the color legend of the map. The segments with orange color background represent high topography regions, while the segments with blue color background represent low topography regions.

Source of data

The data used for this study are six aeromagnetic sheets; 286, 287, 288, 300, 301 and 302 that represent Illushi, Nsukka, Igumale, Onitsha, Udi and Nkalagu areas, respectively. The six data sheets were obtained from Nigerian Geological Survey Agency (NGSA) as an integrated or merged sheet. They were obtained as processed and digitalized data in *XYZ* format. *X* and *Y* are the longitude and latitude measured in metres respectively, while *Z* is the magnetic intensity measured in nanoTesla (nT). The data are part of the new and largest digital airborne data acquired in three phases in most parts of Nigeria between the year 2005 and 2009, by Furgro airborne surveys. The data were acquired by flying an aircraft at 500 m tie-line spacing, 100 m flight line spacing along east–west (E–W) direction and 80 m terrain clearance. Processing and preliminary interpretations were contracted to Paterson, Grant & Watson Limited (PGW) that carried out the geomagnetic gradient removal from raw data using the International Geomagnetic Reference Field (IGRF) formula for 2005. Other preliminary processing of the data includes cultural editing and diurnal variations.

Theory and methodology

The processed and digitized aeromagnetic data in text format data were gridded to form the total magnetic intensity (TMI) map using Oasis montaj software. Various filtering processes were applied using Fast Fourier Transform (FFT) in the spatial frequency domain and different maps were generated. Qualitative and quantitative interpretations were employed in the analyses of this work. The data were qualitatively interpreted majorly for the purpose of delineating the structural lineaments and trends in the study area using the TMI, RTE_INV, vertical derivatives, tilt derivatives (TDR), lineament map, Rose plot and lineament density map.

The total magnetic data were reduced to equator to reduce the magnetic anomalies to the magnetic equator with 0° inclination; as such, re-computes the TMI anomalies as if the causative bodies were magnetized in a horizontal direction. For the convenience of interpretation, a 180° phase reversal was introduced so that troughs become peaks, still positioned over the centers of the bodies (Leu 1981; Pearson and Skinner 1982), hence, the need for reduced to equator
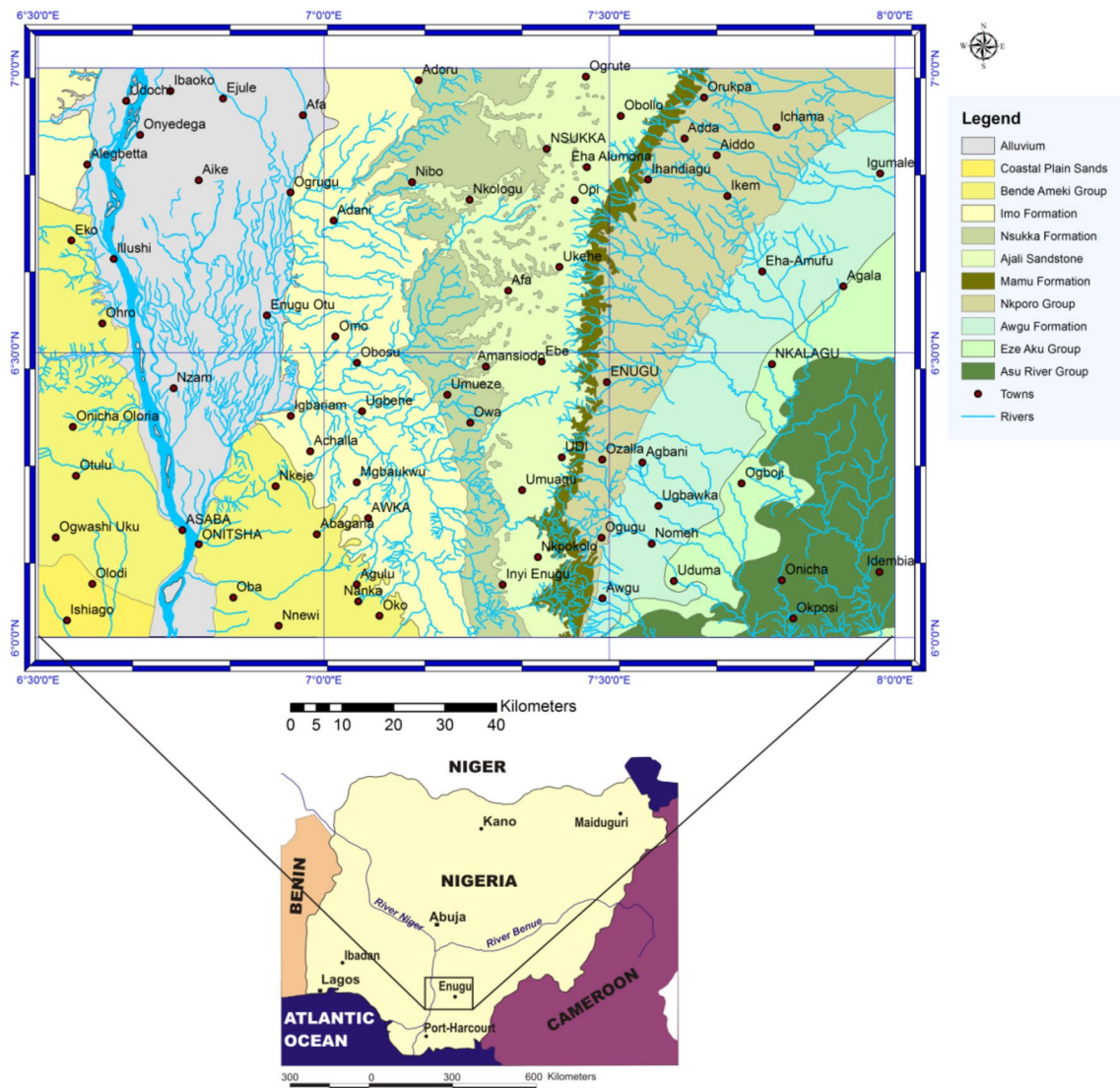
Fig. 1 Location and geology map of the study area

inverse (RTE_INV). Not only that RTE-inverse corrects the effects of low latitude on the magnetic anomaly (Kinnaird et al. 1981; Ngama and Akanbi 2017), but eliminates distortions that would have been introduced in high amplitude anomaly correction if a reduction to pole (RTP) were to be applied. Reduction-to-the-equator filter is well behaved in low and high magnetic latitudes. Oasis montaj software was employed to reduce the data to equator.

First and second vertical (1VD and 2VD) derivatives were applied on the RTE_INV of the TMI using Magmap filtering software imported in Oasis montaj software. The first vertical derivative is equivalent to observing the vertical gradient directly with a magnetic gradiometer. It is a filtering technique that enhances high frequency or short wavelength features (i.e. shallow depth sources) such as dikes, sills, geologic contacts, faults and fractures. The equation for the

computation of vertical derivatives $\left(\frac{\partial^n T}{\partial z^n} \right)$ of the magnetic field data T as shown by Collins (2005) and Hinze et al. (2013) is;

$$F \frac{\partial^n T}{\partial z^n} = k^n F(T) \tag{1}$$

where F is the Fourier representation of the field, k is the wavenumber, and n is the degree of derivatives.

Tilt derivative (TDR) filter was applied on the RTE_INV of the TMI. The TDR filter is good in detecting hidden linear features and characteristically useful in the detection of the edges of the located vertical contacts and other magnetic linear features. Besides, it serves a good purpose in the estimation of depth to vertical contacts. However, the latter purpose is properly integrated in the source parameter

Fig. 2 . Digital elevated model (DEM) of the study area

imaging technique discussed below. TDR is produced by computing the first derivative filter of the tilt angle using Oasis Montaj software.

Mapping of the structural lineament data of the study area was done using the first vertical derivative (1VD) data and employing Oasis Montaj software. To show the relationship between the alignment of the lineaments and magnetic anomalies in the study area, the lineament map was superposed on the tilt derivative (TDR) map using ArcGIS software imported into Oasis Montaj software. The distribution of the lineaments in the study area was interpreted by generating lineament density data and map using the lineament data and employing ArcGIS software. The lineament density data described the lineament cluster or lineament per unit square area in the study area. The lineament density data provide insight into the region of the study area that have the lineament features such as faults, fractures, folds, cracks, contacts, etc., that are potential hosts to mineral deposits and hydrocarbon resources.

The directional attributes or trends of the lineaments are determined by a Rose plot which describes the lineament orientations in the study area. The Rose plot was computed using the lineament data and employing GEORIENT software imported into Oasis Montaj software.

Quantitative interpretations employed in this study are source parameter imaging (SPI) and Euler deconvolution techniques. Source parameter imaging technique is a refinement of the complex analytical method used in quantitative estimation of the location and depth of vertical magnetic source without prior information on the source configuration. SPI requires second derivatives of the anomaly field, employs a local wavenumber, k, term to determine the depth to 2D magnetic sources. SPI depth to magnetic source estimate is represented mathematically (Thurston and Smith 1997) as;

$$\text{Dept} = \frac{1}{k_H} = \frac{1}{\left[\frac{\delta T}{\delta H}(\text{tilt angle}, \theta)\right]} \tag{2}$$

k_H is the derivative of the change in phase in the horizontal plane of x and y.

Tilt angle is a generalized definition for local phase (Verduzco et al. 2004) defined as;

$$\theta = \tan^{-1}\left(\frac{\delta T/\delta Z}{\delta T/\delta H}\right) \tag{3}$$

where

$$\frac{\delta T}{\delta H} = \sqrt{\left(\frac{\delta T}{\delta x}\right)^2 + \left(\frac{\delta T}{\delta y}\right)^2} \tag{4}$$

T is the total magnetic intensity (TMI), while $\frac{\delta T}{\delta x}$, $\frac{\delta T}{\delta y}$ and $\frac{\delta T}{\delta z}$ are the first-order partial derivatives of total magnetic

field intensity (*T*) in *x*, *y* and *z* coordinates. SPI depth estimation is independent of the magnetic inclination, declination, dip, strike and remnant magnetization. For a 2D vertical contact that is vertically polarized, the tilt angle which ranges between ± 90° is zero directly over the contact (Salem et al. 2007), thus locating the position of the contact. Furthermore, the horizontal distance from the 45° to the 0° position of the tilt angle is equal to the depth to the top of the contact. However, assumption requires that the magnetic field be reduced-to-the-pole (or reduced to equator-inverted) and that the remnant magnetization of the source be negligible. Although, as it is the case with other methods, results are subject to an error where the anomaly patterns of contacts interfere with each other, the method is advantageous because it is not dependent on higher-order derivatives, and thus is less subject to noise than other methods requiring higher-order derivatives.

Additionally, the method uses normalized values based on the ratio of derivatives, so it is particularly suitable to situations where both shallow and deep sources are being investigated or where the magnetic anomaly amplitude varies over a wide range owing to extreme variations in the magnitude of the magnetic moment of the sources. SPI map was generated by using RTE_INV of the TMI and employing SPI plug-in in Oasis montaj software.

Euler deconvolution technique is used to discriminate or analyze anomalies from magnetic sources, based on the geometric description of the anomaly sources. It employs Euler homogeneity equation that relates the magnetic field and its gradients components to the location of the source, with the degree of homogeneity, n, which may be interpreted as a structural index, S.I., (Thompson 1982). The basic equation of Euler deconvolution as given by Thompson (1982) is;

$$\left(x - x_0\right)\frac{\delta T}{\delta x} + \left(y - y_0\right)\frac{\delta T}{\delta y} + \left(z - z_0\right)\frac{\delta T}{\delta z} = n(b - \phi) \quad (5)$$

where (x_0, y_0, z_0) is the position of the magnetic source whose total field anomaly *T* is detected at the position *x, y* and *z*. The total field anomaly *T* has a regional value of b. The method assumes simple geometries such as spheres or compact bodies ($n = 3$), line source, narrow pipe, vertical and horizontal cylinders ($n = 2$), thin sheet edge or sill and dyke ($n = 1$), and the vertical edges or contact ($n = 0$) of thick slabs. Euler deconvolution map in this study was carried out using RTE_INV of the TMI and employing the Euler plug-in in Oasis montaj software.

Results and discussion

The TMI map of the area (Fig. 3) produced anomalies that indicate an apparent structural trend in NE–SW and NW–SE directions. The magnetic intensity values range from − 300 to 200 nT. The magnetic variation in the TMI values is a possible attribute of any or more of the following; variation
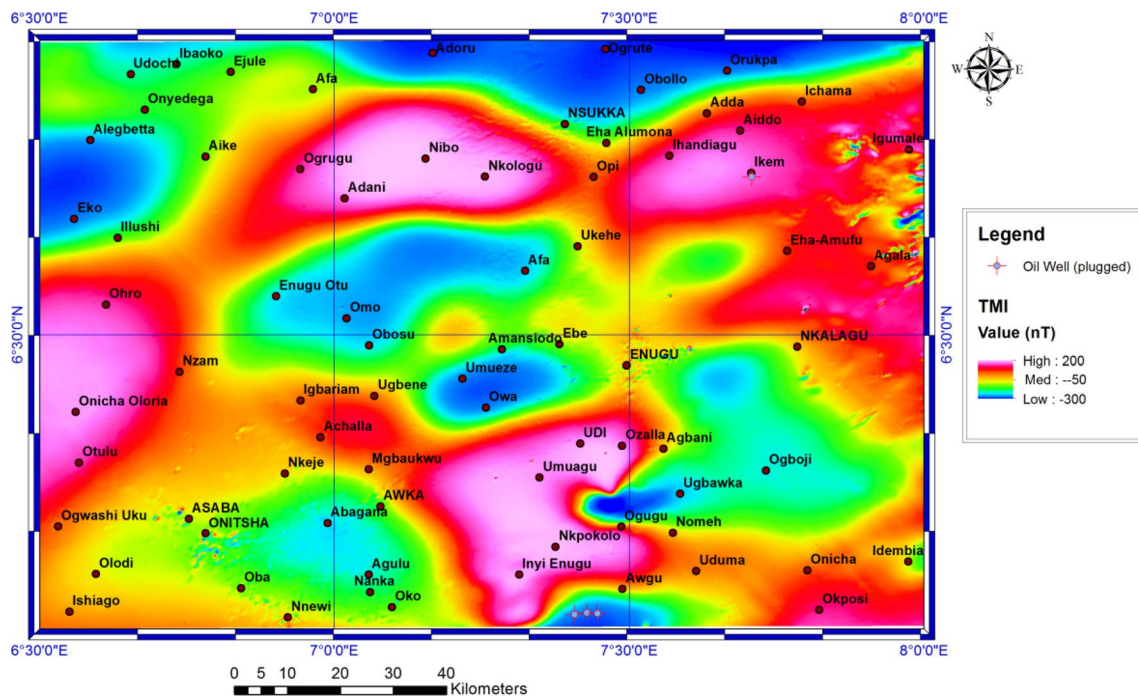

Fig. 3 Total magnetic intensity (TMI) map of the study area

in lithology, the difference in depth of magnetic sources, susceptibility contrast and degree of the strike. Further simplification of the interpretation of the TMI anomalies was done by correcting the TMI for magnetic inclination using the RTP (Fig. 4), RTE (Fig. 5a), and RTE_INV (Fig. 5b). A comparison between the RTP and RTE_INV maps shows that RTE_INV which is an inverse of the RTE displays clearer definitive anomalies than the RTP map. The noise observed in RTP map is perhaps due to the amplitude correction error of the RTP.

Reduction-to-equator inverse (RTE_INV) map (Fig. 5b) has correctly centered the peaks over the corresponding magnetic anomaly sources without image distortions. The magnetic anomalies values of RTE_INV map (Fig. 5b) range from − 155 to 208 nT as indicated by the colour legend bar. The high magnetic anomalies trend mainly in the NE–SW direction in most parts of the basin and in the E–W directions in the uppermost part of the study area. The first and second vertical derivatives (1VD and 2VD) displayed in Fig. 6a and b were performed to reduce the complexity of anomaly and to display clearer imaging of the causative structures than the TMI and RTE_INV. Comparison between 1 and 2VD maps indicates that the second vertical derivative map displays more shallow features but with a lot of noise signals that mask the structural edges of the anomalies. The 1VD map shows better resolution of closely spaced sources with strong appearances of shallow magnetic features that have sharp edges. They are located mainly in the northeast,

northcentral, southcentral and southwest regions of the basin.

The range of values of the magnetic gradient of the basin is − 0.3588 to 0.1675 nT/km. The lower values indicate the possible presence of deep features while the higher values show the possible presence of shallower structural magnetic features such as shallow cracks, joints, fracture, faults, etc.

The lineament map (Fig. 7) of the study area shows structural lineaments of different orientations and varied lengths. The number of lineaments estimated from the map using the ArcGis software of Oasis Montaj is 571. In addition, the ranges of the various lengths of the lineaments were estimated to be between 2.35 km and 103.69 km. The TDR map (Fig. 8) shows clear edge detection of the low and high magnetic anomalies that mostly trend in NE–SW, E–W and NW–SE directions. In addition, the TDR map shows some tiny shallow features that are traced from the central region to the southwest region of the study area. The appearance of these tiny features in the TDR map is consistent with that shown in the 1VD and 2VD maps (Fig. 5a and b). When the lineament map (Fig. 7) was superposed on the TDR map (Fig. 8), lineament—TDR superposition map (Fig. 9) was obtained. The lineament—TDR supposition map shows some reasonable correlations between the alignment of the lineaments and the edges of occurrence of magnetic anomalies. From the map, there is a good relationship between the positions of the high occurrence of the lineaments and the edges of magnetic
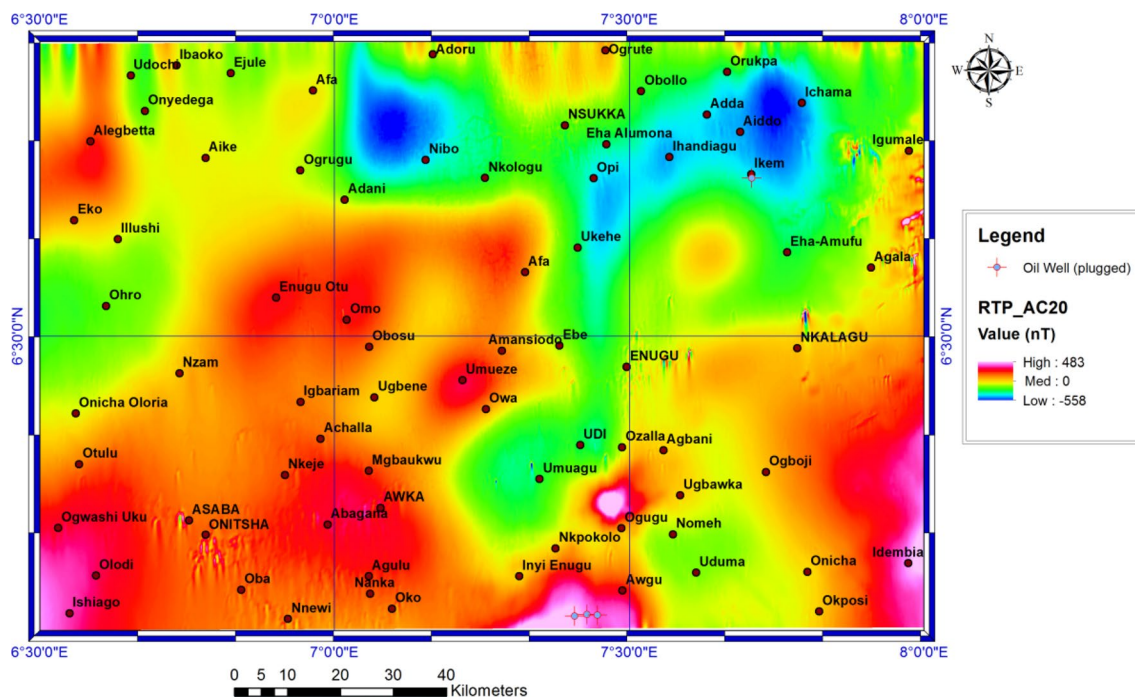

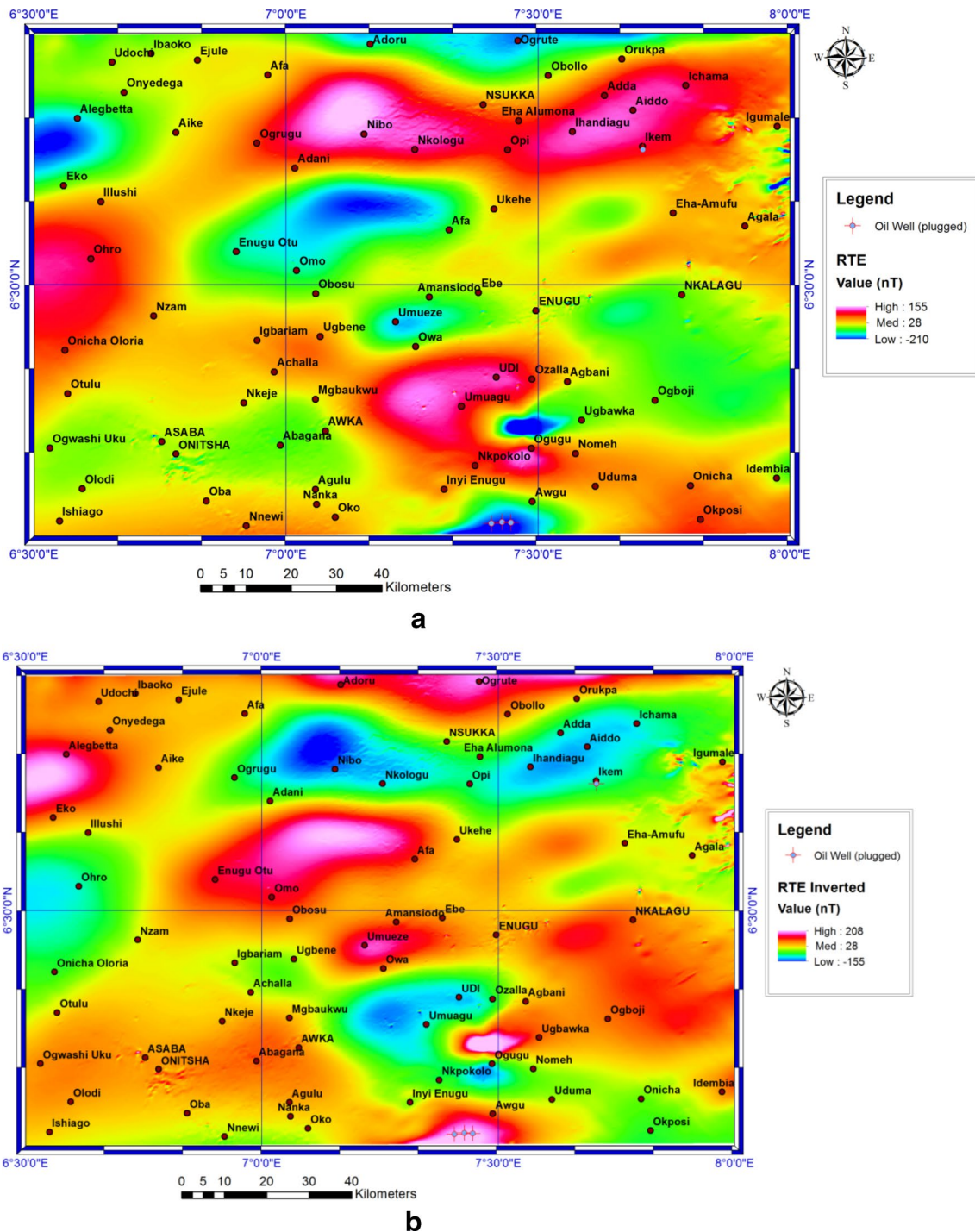**Fig. 4** Reduction to equator (RTP) map of the study area

Fig. 5 **a**. Reduction to equator (RTE) map of the study area. **b** Reduction to equator inverse (RTE-INV) map of the study area

anomalies. Most of the lineaments align along with the trends of the high magnetic gradients indicated by pink and red colour aggregate; while very few of the lineaments are located along the low magnetic gradients indicated by blue and lemon colours.

The implication of these results is that the structural lineaments are perhaps responsible for the high magnetic anomalies in the TDR map of the study area.

The lineaments were classified in accordance with their directional attributes using Rose plot (Fig. 10), produced by

a

b
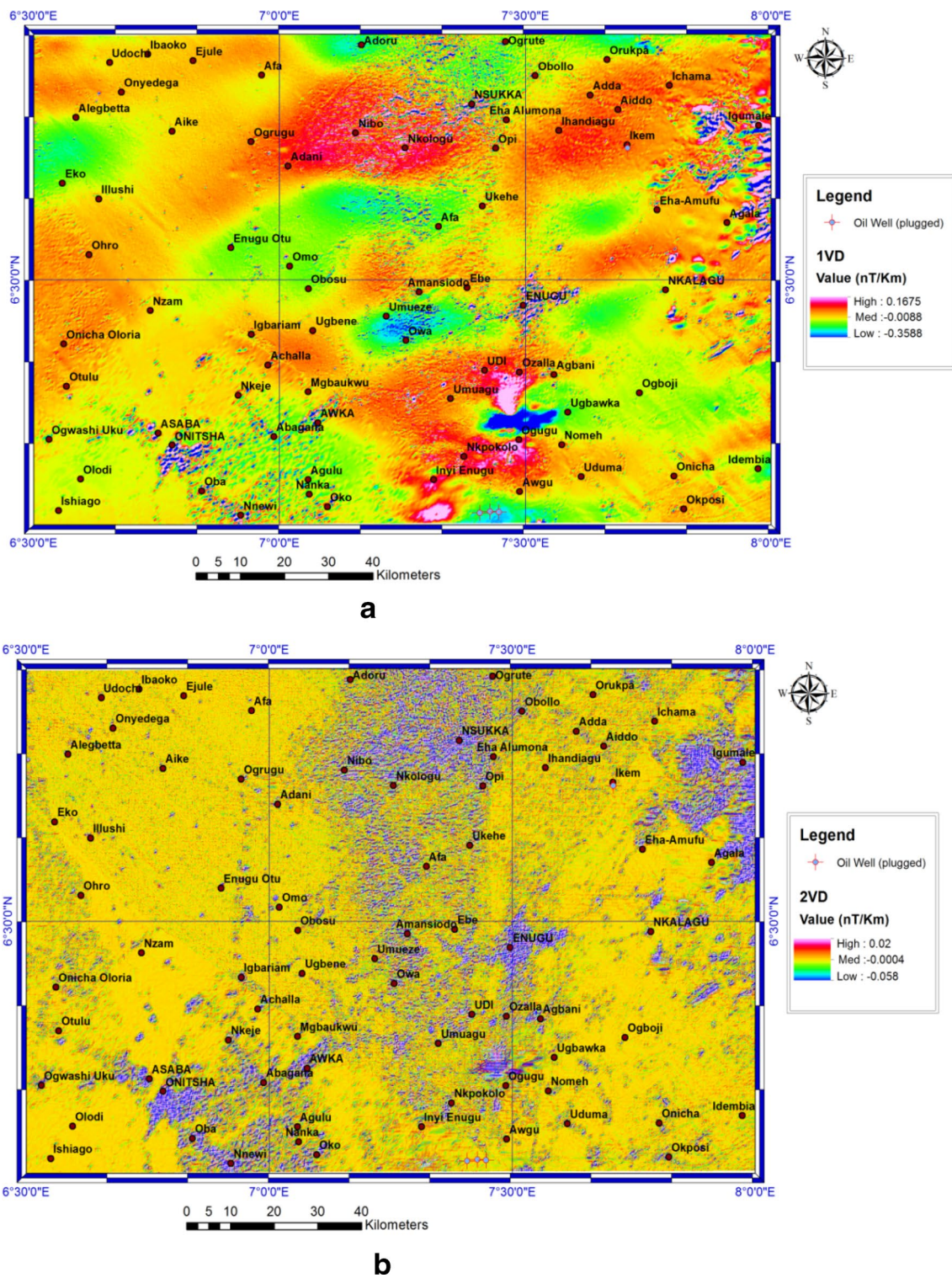
Fig. 6 **a**. First vertical derivative map of the study area. **b**. Second vertical derivative map of the study area

employing Oasis Montaj software. The Rose plot reveals a dominant NE–SW trend with ancillary trends in E–W, NW–SE and N–S directions. Others include NNE-SSW and ENE–WSW trends. Lineament density map (Fig. 11)

of the study area shows lineament density ranging from 0 to 50,000 m^{-3}. The high lineament density values shown in red boxes are more abundantly located in the northeast and northwest regions of the study area. Except for a high
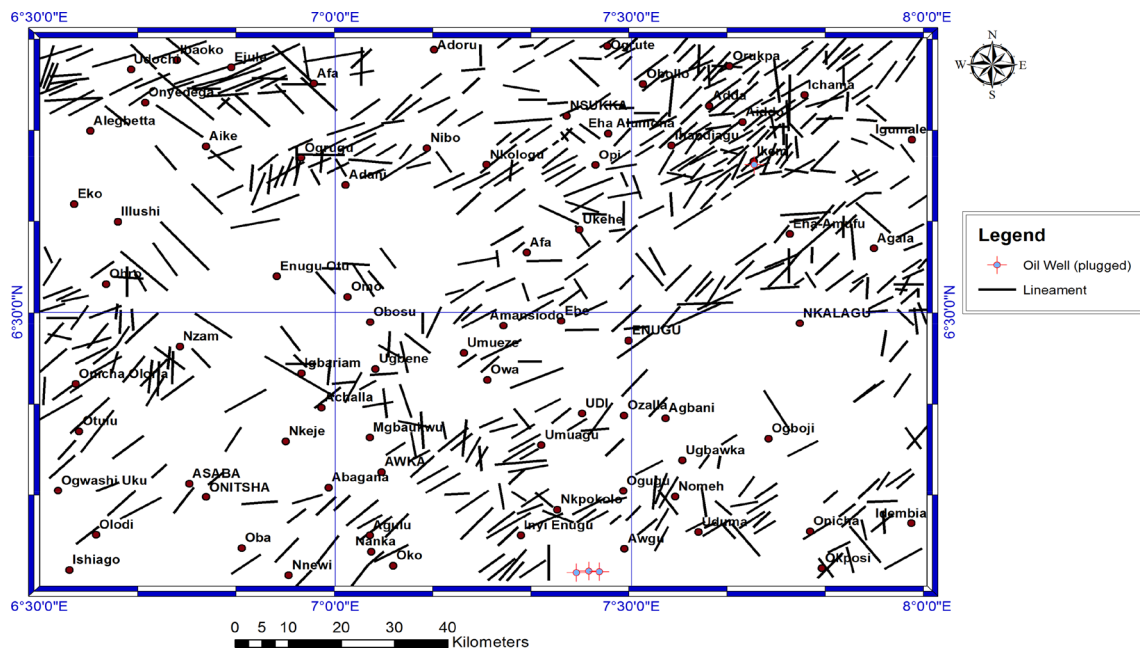
Fig. 7 Lineament of the study area
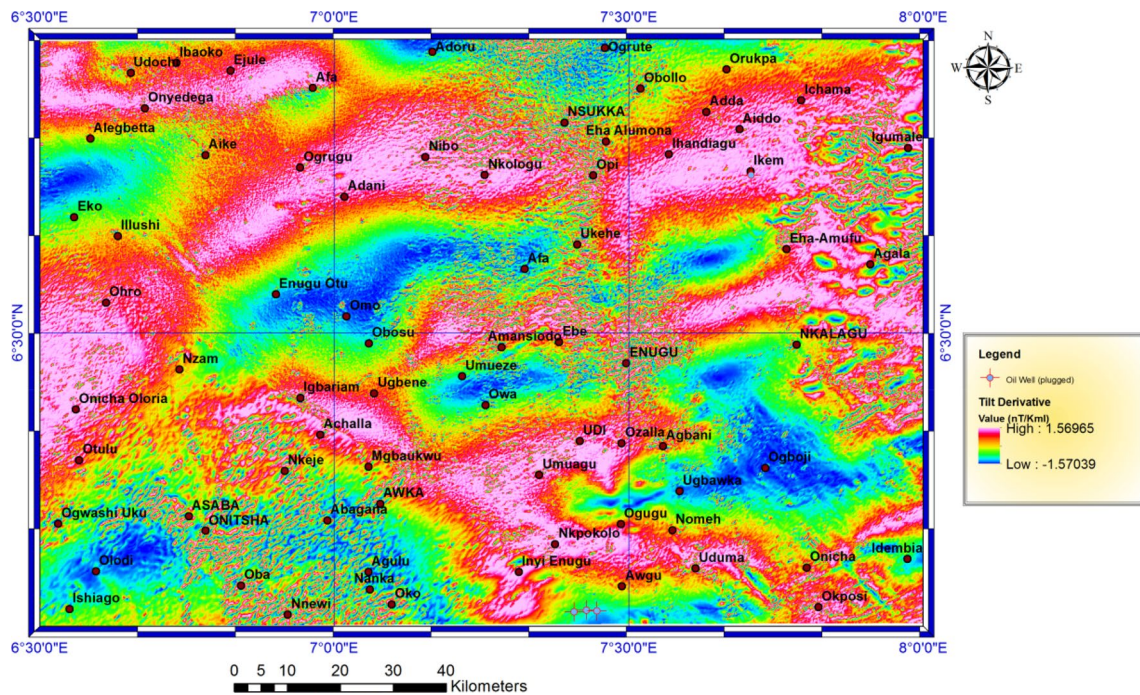
Fig. 8 Tilt derivative (TDR) map of the study area

lineament density location near Awka in the southcentral region, the whole of the southern part is characterized by low lineament density shown in blue and lemon boxes. This result is an indication that the lineament structures are more abundant in the northeast and northwest regions of the study area.

The source parameter imaging (SPI) map (Fig. 12) shows varied colours that indicate different depth values of the magnetic source bodies, ranging from 318.45 to − 6000 m for shallow magnetic sources and − 6000 m to − 11,253 m for deep magnetic sources. The positive depth values are marked by the pink and red colour legends that represent
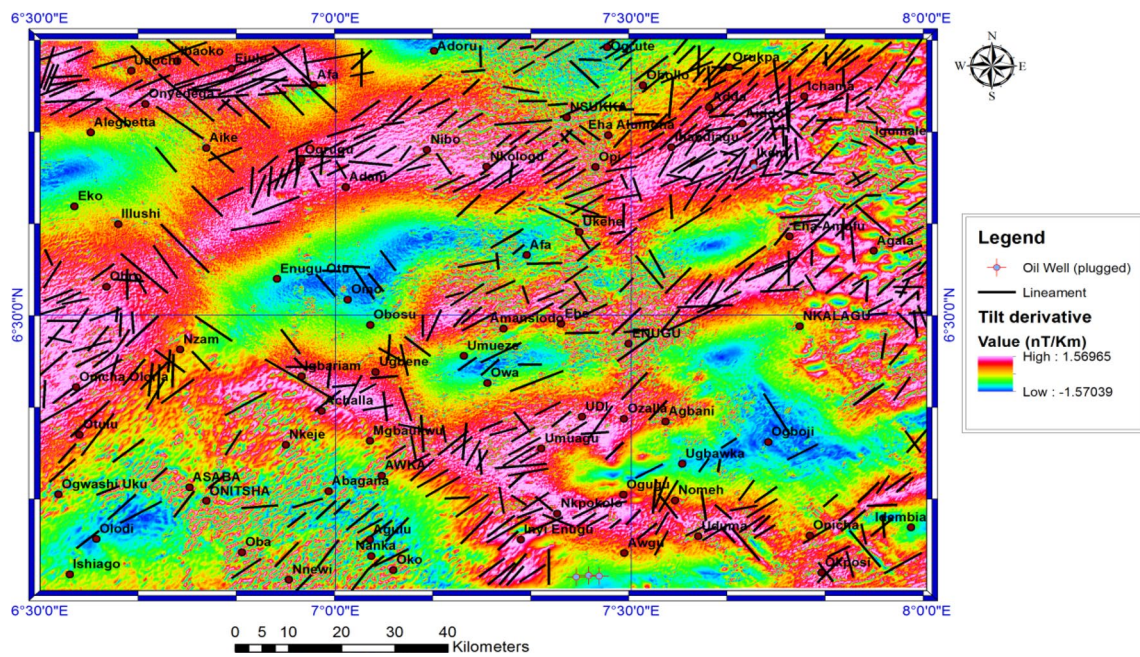
Fig. 9 Lineament-TDR supposition map of the study area

Axial (non-polar) data
No. of Data = 571
Sector angle = 10°
Scale: tick interval = 5% [28.6 data]
Maximum = 18.6% [106 data]
Mean Resultant direction = 053233
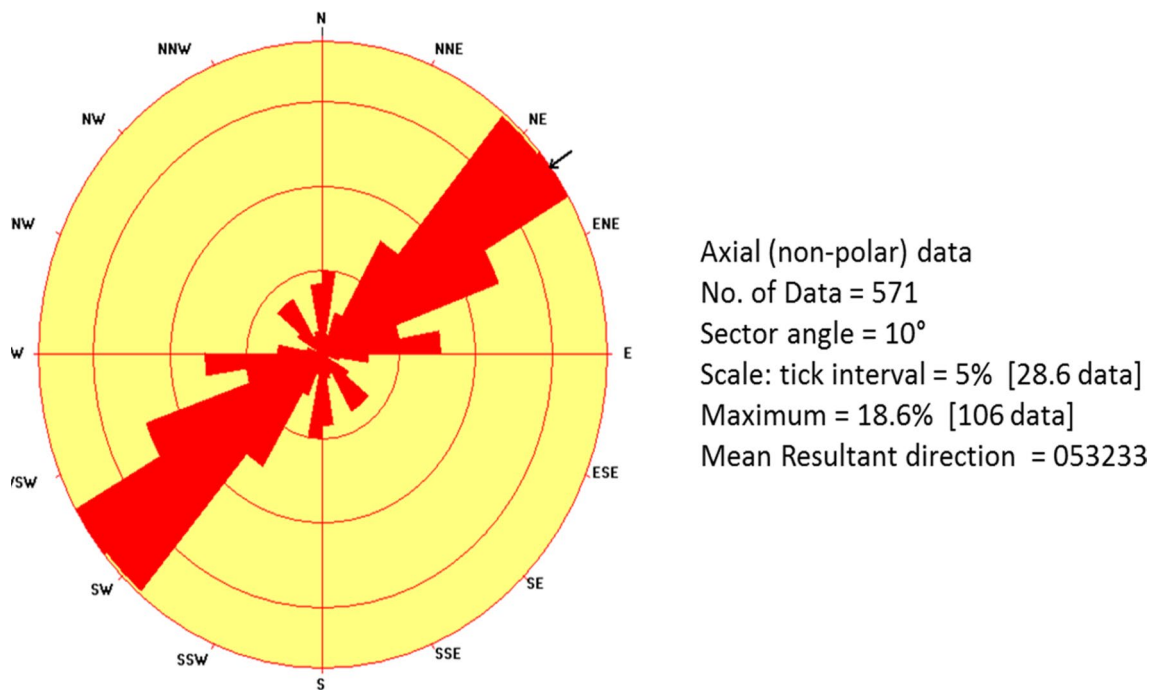
Fig. 10 Rose plot showing the lineament orientations of the study area

locations of outcrops or near-surface intrusive magnetic sources (e.g. lateritic bodies and other shallow magnetic sources). The negative depth values are marked by the blue colour legend that represents the depths of the deep magnetic sources (including deep-seated faults and crystalline basement topography).

Different structural indices were tried on the data and it was discovered that the structural indices, S.I = 0, 1, 2 and 3 provided Euler deconvolution solution that reflected the geological information of the area. The Euler deconvolution map (Fig. 13) shows Euler solutions for the structural index (S.I) values 0, 1, 2 and 3 that represent geological magnetic
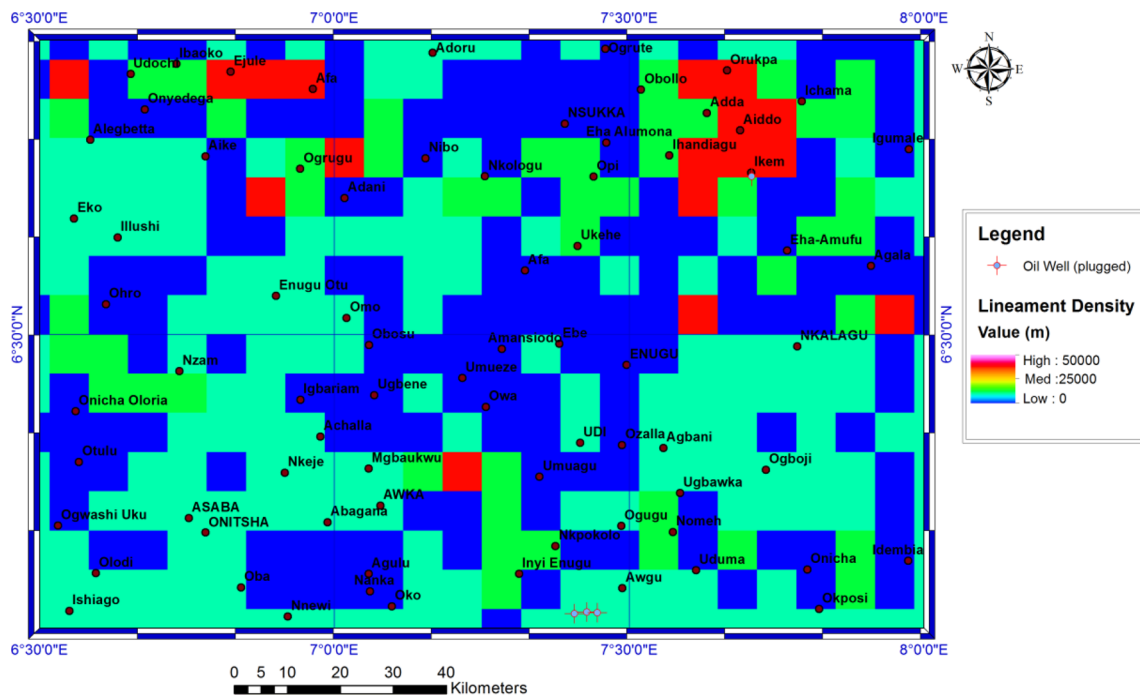
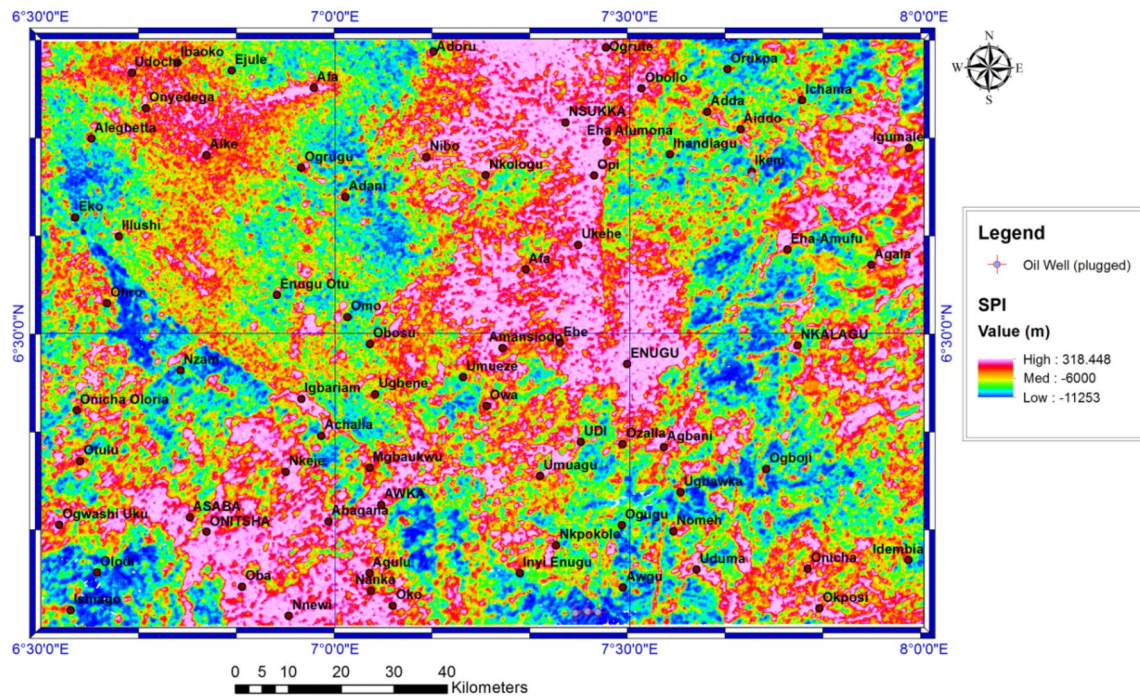**Fig. 11** Lineament density of the study area

Fig. 12 Source parameter imaging map of the study area

models for contact, dyke, horizontal cylinder, and sphere (or compact body), respectively. The different colours in the images represent the depth positions of the magnetic bodies. The blue colour indicates locations for deep-lying magnetic bodies while pink and red colours indicate the locations for the shallow or near-surface magnetic bodies. The colours in-between blue and pink represent locations of magnetic bodies whose depths are between that of deep and shallow
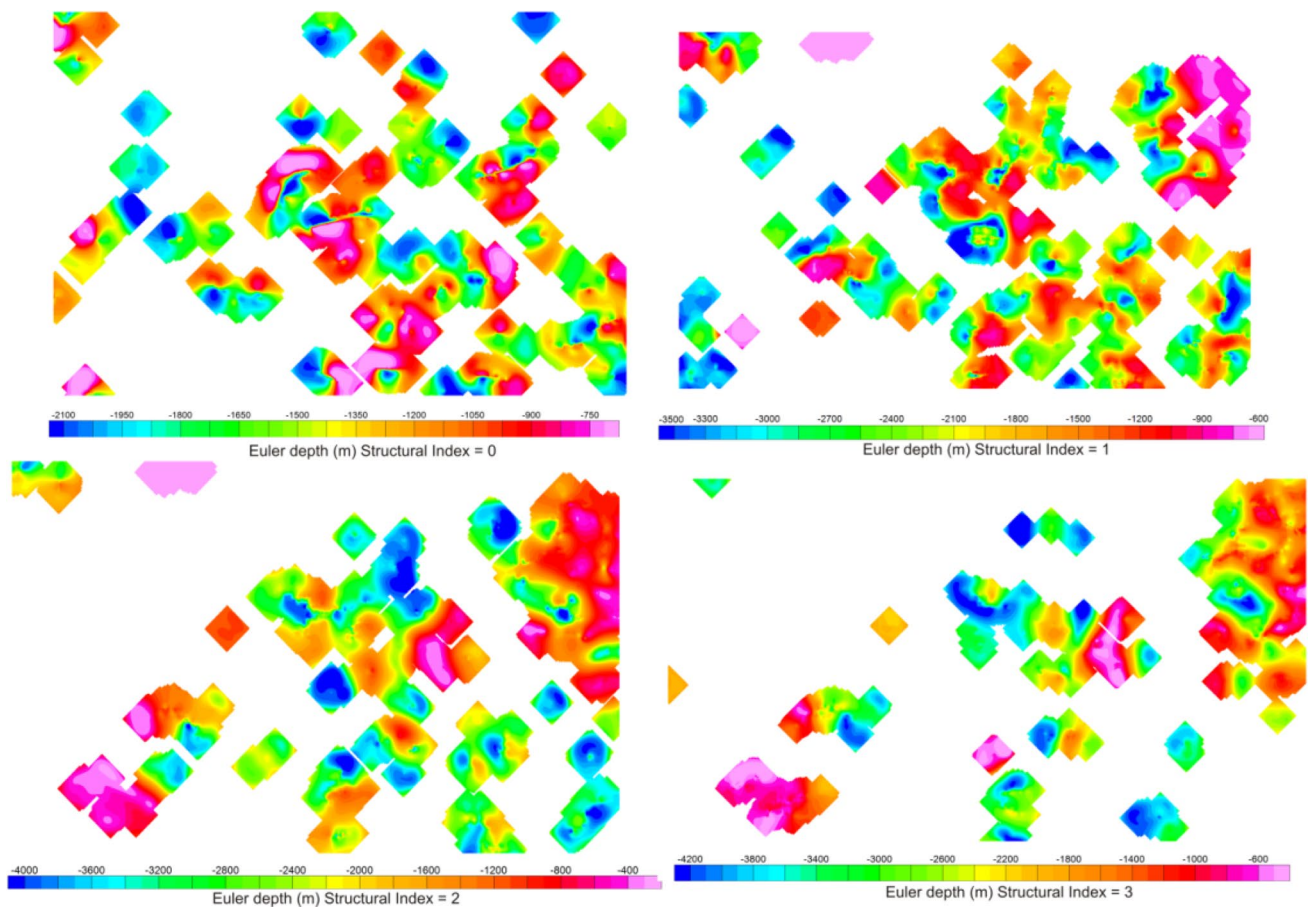
Fig. 13. 3D Euler deconvolution of the study area for structural index 0, 1, 2 and 3

magnetic bodies. Some portions of the map with no colour magnetic signatures or cluster lack Euler depth solution for each of the structural index values. The extreme part of the northeast of the study area shows consistency with the appearance of shallow magnetic sources in the map of S.I. = 1, 2 and 3. The Euler solutions show depth estimates of − 675 to − 2137.5 m for S.I = 0, − 675 to − 3450 m for S.I. = 1, − 400 to − 4100 m for S.I. = 2 and − 500 to − 4300 m for S.I. = 3. The result shows that magnetic bodies with simple geometries such as vertical edges or contact, thin sheet edge or sill and dyke, vertical and horizontal cylinders and spheres or compact bodies are emplaced in the subsurface within the average depth range of − 400 to − 4300 m.

The variations in TMI suggest the attributes of several factors including variation in lithology, the difference in depth of magnetic sources, susceptibility contrast and degree of the strike. From the lineament mapping and the Rose plot, the dominant NE–SW trends might have coincided with the major structural trend of the Benue Trough and would have led to the splitting and drifting apart of the earth's crustal plate; forming a structural earth depression

that gave rise to the sedimentary basin known as Anambra Basin. Also, the event would have generated cracks, folds, fractures, faults and other structural possibilities within the basin that accounts for the ancillary structural lineaments and their trends revealed in this study. The lineaments could be favorable structures that control the mineral deposits in the basin. The result is to a large extent consistent with the earlier result by Ofoha (2015), who studied the structural framework of parts of Anambra Basin and reported trends in NE–SW, NW–SE, NNE–SSW and N–S directions. However, additional structural trends E–W and ENE–WSW were revealed in this study which suggested further tectonic events in the basin. The northeast and northwest regions of the study area with high lineament density suggest regions with more abundance of faults, fractures, lithologic contacts, folds, cracks and other linear features which are possible locales for mineral or hydrocarbon resources. The low lineament density locations (mostly the southern part of the area) may be attributed to mostly fracture lines that might have been formed due to the tensional stresses. The result agrees with that of Ananaba and Ajakaiye (1987) and Megwara and

Udensi (2014) that had earlier linked lineament density to mineralization.

The possibility of the appearance of fractures suggests that the study area is also a potential aquifer repository (Megawara and Udensi 2014; Abdullahi et al. 2013). Lineaments like joints, fractures, etc., developing generally due to tectonic stress and strain, provide an important clue on surface features and are responsible for the infiltration of surface run off into subsurface and also for movement and storage of groundwater (Abdullahi et al. 2013).

SPI depth result revealed a total depth range between 318.45 and 11,253 m. Earlier, Anyadiegwu and Ijeh (2018) reported SPI depth result between 0.1883 km for shallow magnetic bodies and 8.0683 km for deep-seated magnetic bodies of aeromagnetic data of Nsukka, Udi, Nkalagu, and Igunmale areas. Perhaps, the slight difference in the depth result of this study and that of Anyadiegwu and Ijeh (2018) may be attributed to the difference in the area of coverage by both studies. The scope of the present study is quite larger than the earlier study by Anyadiegwu and Ijeh (2018). The SPI shallow depth results (ranging from 318.45 to − 6000 m) and the 3D Euler deconvolution depth result (ranging from − 400 to − 4300 m) revealed the depth emplacement of the shallow magnetic sources including the outcrops and the lineament sources. The positive depth values depict the outcrops shown as a conical shaped high topography passing from the northcentral to southcentral region of the basin (Figs. 2 and 12). The negative depths values are the possible locations of the shallow magnetic lineaments that perhaps indicate shear zones, veins, lithologic boundaries, dykes, etc. Geological information of the basin gives credence to the evidence that the lithologic boundaries suggest the possible occurrence of lithologies such as shale, sandstone, siltstone, coal, subordinate limestone in some parts of the basin as reported by Nwajide and Reigers (1996). The sandstone is mineralogically mature for minerals such as quartz, micas, zircon, gypsum, tourmaline and magnetite which are all forms of dykes (Nwajide and Reigers 1996).

The SPI maximum depth (− 11,253 m) revealed a sedimentary thickness that is sufficient enough for hydrocarbon maturation. Wright et al. (1985) reported that the minimum sedimentary thickness required for commencement of oil formation from organic remains would be 2.3 km deep.

Conclusion

Aeromagnetic data of some parts of Anambra Basin were interpreted to delineate the subsurface structural lineaments and their corresponding trends, and to estimate the depths to anomalous magnetic sources. The structural lineaments and trends of the study area were delineated by employing reduction to equator-inverted, first vertical derivatives, tilt derivative, lineament data, Rose plot and lineament density data. The depth to the magnetic sources was determined using source parameter imaging and deconvolution techniques. 571 structural lineaments that have varying lengths between 2.35 and 103.69 km were delineated. The trends of the lineament are dominant in NE–SW trend, with ancillary trends in EW, NW–SE and NS directions. Others include NNE–SSW and ENE–WSW trends. Northeast and northwest of the study area have more lineament density and predict areas of potential hosts to both mineral deposits and hydrocarbon resources. The SPI depth ranges from 318.45 to − 6000 m for shallow magnetic sources and − 6000 to − 11,253 m for deep magnetic sources and the 3D Euler deconvolution revealed magnetic bodies that are emplaced at the depth between − 400 and − 4300 m. The vast presence of lineaments in the study area suggests the existence of faults, fractures, shear zones, veins, lithologic boundaries, dykes, etc., that suggest potential hosts to source mature rocks such as clay, magnetite, hematite, pyriotite, gypsum and other numerous magnetic minerals that will encourage mineralization in the Basin. Also, they are structural possibilities that may enhance the migration and entrapment of hydrocarbon in the sediments. The depth result has also shown good evidence for hydrocarbon maturation. Government should encourage vigorous research and exploration in the Basin by providing healthy policies and supports to intending researchers and local potential investors.

References

Abdullahi BU, Rai JK, Momoh E, Udensi EE (2013) Effect of lineaments on groundwater occurrence. Int J Environ Bioener 8(1):22–32

Adeigbe OC, Salufu AE (2009) Geology and depositional environment of Campano-Maastrichtian sediments in the Anambra Basin, Southeastern Nigeria: evidence from field relationship and sedimentological study. Earth Sci Res J 2(13):148–166

Adetona AA, Abu M (2013) Estimating the thickness of sedimentation within Lower Benue Basin and Upper Anambra Basin, Nigeria, using determination and source parameter imaging. Geophys (Hindawi Publ Company) A12706:1–10

Aigbogun C, Olorunsola K (2018) Determination of curie point depth of Anambra Basin and its environs, using high resolution airborne magnetic data. IJRRAS 34(2):47–54

Ananaba SE, Ajakaiya DE (1987) Evidence of tectonic control of mineralization in Nigeria from lineament density analysis A Landsat-study. Int J Remote Sensing 8(10):1445–1453

Anyadiegwu C, Ijeh IB (2018) Depth to magnetic source analysis using source parameter imaging (SPI), analytical depth and spectral depth estimates. Umudike J Eng Technol 4(1):124–134

Collins R (2005) Aeromagnetic surveys principles, practice and interpretations. Geosoft, Netherlands

Ekine SE, Onuoha KM (2008) Burial history and subsidence in the Anambra Basin Nigeria. Nigerian J Phys 20(1):145–154

Ekweozor CM (2006) Searching for petroleum in the Anambra Basin, Nigeria. In: Okogbue CO (ed) Hydrocarbon potentials of Anambra Basin. Great AP Express, Nsukka, pp 47–82

Ekwueme OU, Obiora DN, Igwe EA, Abangwu JU (2018) Study of aeromagnetic anomalies of Idah and Angba areas, north central Nigeria, using high resolution aeromagnetic data. Model Earth Syst Environ 4:461–474

Farah D, Mohammad ZK, Delwar H (2009) Analyzing gravity and magnetic data in Surma Basin, Bangladesh. Jahangirnagar Univ J Sci 32(1):19–28

Gunn PJ (1995) An algorithm for reduction to pole that works at all magnetic latitudes. Explor Geophys 26:247–254

Hinze WJ, VonFrese RRB, Saad AH (2013) Gravity and magnetic exploration: principles, practices and applications. Cambridge University Press, New York

Kinnaird JA, Bowden P, Bennett JN, Turner DC, Abba SAB (1981) Geology of the Nigeria anorogenic ring complexes. Jown Bartholomew and Sons Ltd, United Kingdom

Leu LK (1981) Use of reduction-to-the-equator process for magnetic data interpretation. SEG abstract 1:35

Megwara JU, Udensi EE (2014) Structural analysis using aeromagnetic data: case study of parts of Southern Bida, Nigeria and the surrounding basement rocks. Earth Sci Res 3(2):27–41

Ngama EJ, Akanbi ES (2017) Qualitative interpretation of recently acquired aeromagnetic data of Naraguta area, North Central, Nigeria. Journal of Geography, Environment and Earth Science International 11(3):1–14

Nwajide CS (2006) Anambra basin of Nigeria: synoptic basin analysis as a basis for evaluating its hydrocarbon prospectivity. In: Okogbue CO (ed) Hydrocarbon potentials of Anambra Basin. Great AP Express Publishers, Nsukka, pp 47–82

Nwajide CS, Reigers TJA (1996) Geology of the Southern Anambra Basin. In: Reigers, TJA (eds) Selected chapters on geology: Sedimentary geology and sequence stratigraphy in Nigeria and and three case studies and a field guide. SPDC Corporate, Warri, Nigeria

Obiora DN, Ossai MN, Okwoli E (2015) A case study of aeromagnetic data interpretation of Nsukka area, Enugu State, Nigeria, for hydrocarbon exploration. Int J Phys Sci 10(17):503–519

Obiora DN, Ossai MN, Okeke FN, Oha AI (2016) Interpretation of airborne geophysical data of Nsukka area. J Geol Soc India 88(4):654–667

Ofoegbu CO (1984) Interpretation of aeromagnetic anomalies over the lower and middle Benue Trough of Nigeria. Geophys J R Astr Soc 79:813–823

Ofoha CC (2015) Spectral analysis of aeromagnetic anomalies from parts of Mmaku and its adjoining areas in Southeastern, Nigeria. Int J Sci Res Publ 5(10):1–5

Okorie AC, Obiora DN, Igwe E (2019) Geophysical study of Ubiaja and Illushi area in northern Anambra basin, Nigeria, using combined interpretation methods of aeromagnetic data. Model Earth Syst Environ 5:1071–1082

Onwuemesi AG (1997) One-dimensional spectral analysis of aeromagnetic anomalies and Curie depth isotherm in the Anambra Basin of Nigeria. J Geodyn 23(2):95–107

Onyewuchi RA, Opara AI, Ahiarakwem CA, Oko FU (2012) Geological interpretations inferred from airborne magnetic and landsat data: Case study of Nkalagu area, Southeastern Nigeria. Int J Sci Technol 2(4):178–191

Pearson WC, Skinner CM (1982) Reduction-to-the-pole of low latitude magnetic anomalies. SEG Abstr 1:356–358

Reyment RA (1965) Aspect of the geology of Nigeria cretaceous and cenozoic deposits. University Press, Ibadan

Salem A, Williams S, Fairhead J, Ravat D, Smith R (2007) Tilt-depth method: a simple depth estimation method using first-order magnetic derivatives. Lead Edge 26:1502–l505

Thompson DT (1982) EULDPH—new technique for making computer assisted depth estimate of magnetic data. Geophys 47:31–37

Thurston JB, Smith RS (1997) Automatic conversion of magnetic data to depth, dip, susceptibility contrast using the SPITM method. Geophysics 62:807–813

Verduzco B, Fairhead JD, Green CM, Mackenze C (2004) New insights into magnetic derivatives for structural mapping. Lead Edge 23:116–119

Whiteman AJ (1982) Nigeria: Its petroleum geology potential. Graham and Trotman, London

Wright IB, Hastings D, Jones WB, Williams HF (1985) Geology and mineral resources of West Africa. George Allen and Urwin, London

Yakubu JA, Okeke FN, Obiora DN (2020) Estimation of Curie point depth, geothermal gradient and heat flow within the lower Benue trough, Nigeria using high resolution aeromagnetic data. Model Earth Syst Environ 2:2. https://doi.org/10.1007/s40808-020-00760-7